JOURNAL OF OPTOELECTRONICS AND ADVANCED MATERIALS Vol. 10, No. 8, August 2008, p. 2028 - 2032

Application of dielectric barrier discharge for plasma polymerization processes

I. TOPALA[*a,b], M. ASANDULESA[a], N. DUMITRASCU[a], G. POPA[a], J. DURAND[b]
[a]*Plasma Physics Department, Faculty of Physics, "Al. I. Cuza" University, Blvd. Carol I, No. 11, 700506 Iasi, Romania*
[b]*Institut Européen des Membranes, Université Montpellier II, CC 067 Place Eugène Bataillon, 34095 Montpellier, France*

A new technique based on plasma polymerization at atmospheric pressure is presented in obtaining thin functional polymers films. A dielectric barrier discharge (DBD) is used to initiate the polymerization reaction of two monomers, acrylic acid (AAc) and N-vinyl formamide (NVF) as a source of hydroxyl and amino functionalities in the structure of the films. The discharge diagnosis was performed by electrical measurements and spatially resolved optical emission spectroscopy (OES). The wettability of polymer films was analysed by contact angle measurements and the chemical structure by attenuated total reflectance Fourier transform infrared (ATR-FTIR) spectroscopy. The experimental data proved that our DBD is working in the homogenous regime and the reactive species, such as molecular nitrogen and atomic oxygen, are presented in the discharge volume. The estimations of gas temperature given values around 340 K, concluding that thermal effects are excluded in the polymerization process. The DBD plasma exposure of PET films makes them more wettable, the water contact angle decreasing from 79° to 42°. After the polymerization reaction, the water contact angle was 20°, values corresponding to the deposited polymerised films. Based on ATR-FTIR spectra they were identified OH and NH functional groups in the chemical structure of plasma polymerized films.

(Received March 1, 2008; accepted June 30, 2008)

Keywords: Acrylic acid, N-vinyl formamide, Polymerization, Dielectric barrier discharge

1. Introduction

In the treatment of acute lymphoblastic leukemia a wide number of therapeutic solutions are now available, including chemotherapy and radiotherapy. Among the chemotherapeutic agents, the L-Asparaginase has good results. This is an enzyme which catalyzes the hydrolysis reactions of Asparagine into Aspartic acid with ammonia as byproduct. On the other hand, the leukemia cells are characterized by their incapacity to synthesize the Asparagine. As result, by the L-Asparaginase administration, the level of Asparagine is decreased in the circulating blood and the tumor cells are rapidly killed. Fortunately, the normal cells have the capacity to synthesize the Asparagine and thus they will not be dramatically affected by the depletion of the Asparagine level in the blood. Nevertheless, the administration of L-Asparaginase directly in the blood circulation has some drawbacks such as the elimination of the active principle by different metabolic pathways and the possibility to induce severe allergic reactions. An alternative to the classic treatment with L-Asparaginase it can be the enzyme immobilization onto polymer substrates, followed by the incorporation in blood contacting devices [1,2].

Nowadays the plasma polymerization technique is used to obtain unique kinds of polymers, significantly different from conventional polymers and which cannot be obtained under classical chemical polymerization conditions. New applications of plasma polymers are developed continuously, especially in the biomedical domain, due to the necessity of intelligent supports for drug delivery or smart biomaterials. By plasma polymerization one may obtain thin polymer films with controllable density of functional groups (e.g. carbonyl, carboxyl, hydroxyl or amino type), these specific groups being important in the materials biocompatibility. In particular, the plasma treatment of polymer surfaces, either by simple plasma exposure or by deposition of films, may be a good solution to modify the surface properties of most commercial polymers, with direct implications on polymer biocompatibility [3-6].

In this paper it present a new technique based on plasma polymerization at atmospheric pressure, with the aim to obtain thin functional polymers films as support for enzyme immobilization.

2. Experimental

The plasma polymer films have been deposited using a DBD working at atmospheric pressure in plan-plan geometry, with electrodes as stainless steel discs (25 mm diameter). The discharge gap is fixed at 5 mm and the experimental arrangement is presented in Fig. 1. Helium was selected as working gas, being known for its effects on stabilization of electrical discharges at atmospheric pressure and the efficiency in surface modification of polymers. The high voltage electrode presents a "shower head" design, with the principal gas flux oriented to the dielectric barrier. The discharge is driven by a high voltage source, with voltage and current probes connected to a digital scope (LeCroy 434). Using a spatially resolved

acquisition system and an optical fiber connected to a Triax 550 monochromator, the discharge emission spectra can be recorded and analyzed at any position between the electrodes. The monochromator entrance slit has 30 μm and the grating has 600 grooves/mm or 2400 grooves/mm (required for the rotational spectra acquisitions). The total light emission intensity from the DBD discharge was analyzed using a Hamamatsu R955 photomultiplier (spectral range between 160-900nm).

The applied voltage (U_{app}) was varied in the range 3 - 5 kV aiming to obtain different dissipated power in the discharge volume.

The monomer vapors are introduced in the plasma region using a gas handling system: the helium pathway, with a fixed flow rate (25 mL/min) is used to pass/cross trough the AAc reservoir (purity >99%, Merck) or NVF reservoir (purity >99%, BASF), and then assuring a mixture with the principal flux of helium (100 mL/min). The monomers are kept at room temperature and the substrate of polyethylene terephthalate – PET (Goodfellow Co, 125 μm thick) was used as dielectric barrier.

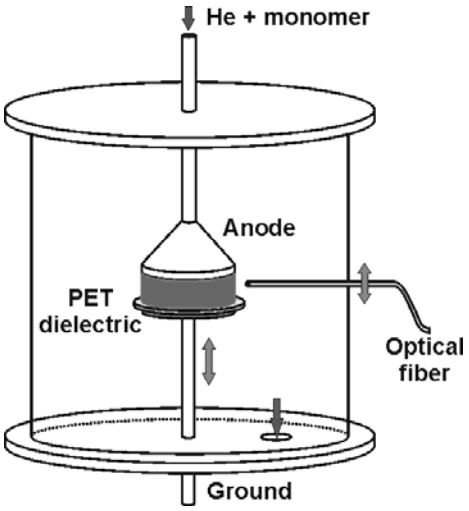

Fig. 1. The DBD reactor used for plasma polymerization at atmospheric pressure: 30 mm diameter disc electrodes, 5 mm gap, dielectric PET 0.125 mm thick.

The plasma polymer films were analyzed by contact angle measurements and FTIR spectroscopy. The contact angles were measured using a digital imaging system. The drop of liquid was deposited onto the sample using a Hamilton syringe and then the photos were taken. The ImageJ open-source software [7] together with the drop analysis plug-in analyzed the images. The FTIR spectra of the plasma polymers films deposited onto the PET substrate were obtained using the attenuated total reflectance (ATR) technique, employing a ZnSe crystal (BioRad spectrometer FTS-60). The presented spectra are the average of 32 scans with 4 cm^{-1} resolution in the 700 – 4000 cm^{-1} range.

3. Results and discussions

3.1. Discharge diagnosis

The time evolution of applied voltage and discharge current signal, also the photomultiplier current are presented in the Fig. 2.

Due to the discharge current evolution as a single sharp peak (at 4.5 μs) it can conclude that our DBD works in the glow mode. As the voltage drops to zero and the internal field inversion occurs, the anode performs role as cathode for a short period of time and a secondary discharge much smaller than the primary discharge [8] appears (at 11.5 μs).

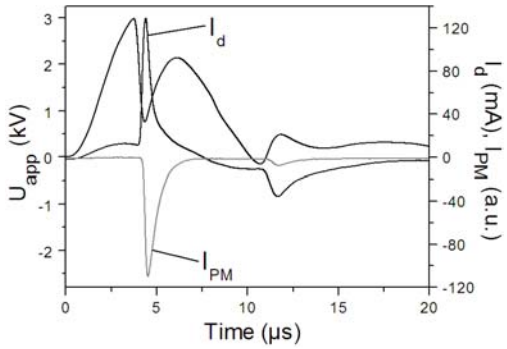

Fig. 2. Signals of applied voltage (U_{app}), discharge current (I_d) and photomultiplier signal (I_{PM}).

The glow mode of the DBD is confirmed also by the spatially distribution analysis of the total light emission intensity in the discharge gap. The glow discharge at low pressure is characterized by an emission intensity distribution with a maximum near the cathode, respectively the negative glow, followed by a relatively constant emission intensity identified as the positive column. In the Fig. 3 it is shown the spatial distribution of the total light emission intensity between the electrodes in the DBD at atmospheric pressure. The integration time of each step was 0.5 s, much larger than the duration of primary and secondary discharges.

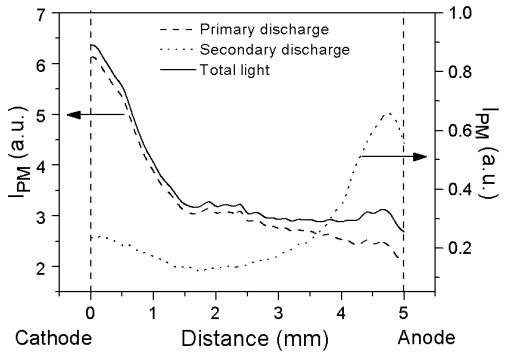

Fig. 3. The spatial distribution of the total light emission intensity in the DBD (U_{app} = 3 kV).

The photomultiplier signals corresponding to the light coming from the primary and the secondary discharge are represented separately, while theirs sum is the total light emission intensity coming from the DBD. Obviously, in case of the primary discharge the most intense region of the DBD is localized near the dielectric, acting as cathode. A decrease in the intensity is registered at 1.5 mm in front of the cathode, followed by a relatively constant region. Related to the secondary discharge, a much smaller intensity it registered with a maximum situated in front of the anode, due to the internal field inversion. In conclusion, the distribution of total light emission intensity in the DBD shows certain similarities with the glow discharge at low pressure. The most intense region of the discharge is located near the cathode, where a maximum of dissipated energy is expected. In this region, they are possible efficient fragmentation processes, followed by deposition and/or polymerization reactions.

A typical emission spectrum of the discharge in helium without monomer vapours is presented in the Fig. 4. The maximum signal is due to the helium $3^3S \rightarrow 2^3P$ transition (706.5 nm). Due to the work at atmospheric pressure it is expected to identify many impurities. Thus, the nitrogen presents bands of the second positive system ($C^3\Pi_u$ - $B^3\Pi_g$) at 337.1 nm, 357.6 nm and 380.4 nm. The molecular ions produced after ionization via Penning processes are excited and identified form the strong emission bands of the first negative system ($B^2\Sigma_u^+$ - $X^2\Sigma_g^+$) at 391.4 nm, 427.8 nm, 470.0 nm. The atomic oxygen lines at 777.4 nm ($3^5P \rightarrow 3^5S$) and 844.6 nm ($3^3P \rightarrow 3^3S$), also a band of OH radical between 306 – 310 nm ($A^2\Sigma^+$ - $X^2\Pi$) have been identified. The above excited species can rapidly participate at chemical reactions in the gas phase and also at the surface, having an important role in knowledge of plasma chemistry.

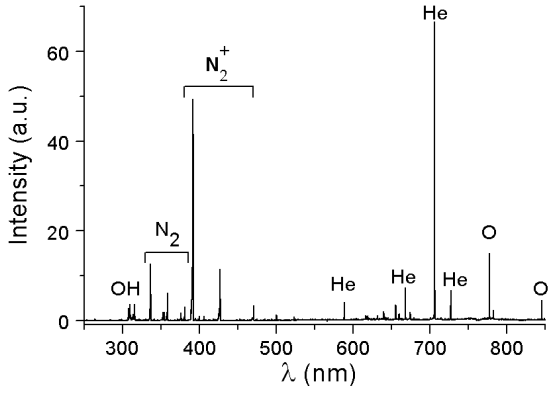

Fig. 4. A typical emission spectrum of the discharge in "pure" helium (U_{app} = 3 kV).

From the signals of applied voltage and the discharge current (Fig. 2) we can observe that the mean pulse duration is less than 1 μs for the primary discharge, and aprox. 1.5 μs for the secondary discharge. During these pulses, in discharge gap many free radicals (neutral particles with mean life time of few ms) are produced and then the plasma vanishes. In this way very efficient chemical reactions involving oxygen and hydroxyl radicals are expected.

The rotational temperature was calculated using the Boltzmann plot method of the line intensities from the R branch of the N_2^+ emission band ($B^2\Sigma_u^+$, v_1=0 - $X^2\Sigma_g^+$, v_2=0) [9]. As discussed in other works, in case of the DBD the rotational temperature can be approximated with the gas temperature [10,11]. Determination of the line intensities and the fitting incertitude induce an error of maximum ±5K. The spatial distribution of the gas temperature is presented in the Fig. 5.

Near the dielectric the mean gas temperature is 340K and a slight increase of the gas temperature was found toward the anode, where the mean value is 380K.

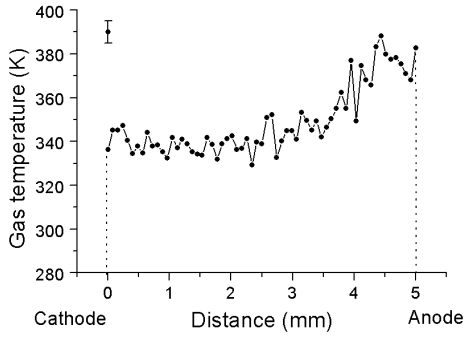

Fig. 5. The spatial distribution of the gas temperature in the DBD. (U_{app} = 3 kV)

3.2. Plasma polymer films characterization

The presence of the functional groups onto the PET substrate due to the deposition of AAc and NVF is proved by measurements of the surface wettability. Thus, if the contact angle of water (θ) onto the untreated PET surface is 79°, on the treated PET is around 42°, proving a more wettable surface after the plasma exposure (Fig. 6). This effect may be explained by the O based functionalities induced the plasma onto the PET surface. As it is shown in the Fig. 6, the variations of θ with the applied voltage appear to be irrelevant.

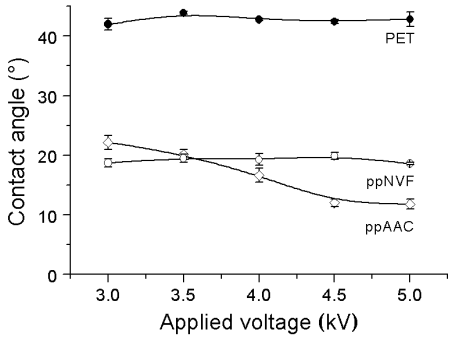

Fig. 6. The water contact angle values for plasma polymers and the substrate.

When the monomer vapours are introduced in the plasma, the PET surface is coated with a thin layer of plasma polymer, the θ giving values around 20°, in the two cases, respectively coatings of ppAAc and ppNVF. In case of ppAAc films a slight decrease of the contact angle values was found with the increase of the applied voltage (Fig. 6). The lower values of the θ onto the deposited plasma polymers confirm the presence of polar groups (hydroxyl, carbonyl and/or carboxyl) incorporated after the plasma action.

By comparison with PET, the FTIR spectra of the deposited plasma films show new absorption bands only in the region of high wavenumbers (2500 – 4000 cm^{-1}) (Fig. 7). This can be explained taking into account the spectra acquisition method by the ATR technique. It is known that the intensity of the IR beam (I) is depending on the wavelength (λ) and decreases exponentially with the depth (z) from the surface [12]:

$$I = I_0 e^{-\frac{z}{d_p}} \quad (1)$$

$$d_p = \frac{\lambda}{2\pi\sqrt{n_1^2 \sin^2\theta - n_2^2}} \quad (2)$$

where I_0 is the intensity of the IR beam at the sample surface (z=0), n_1 is the refractive index of the crystal (2.45 for ZnSe), θ is the incidence angle of the IR beam at the sample – crystal interface and n_2 is the refractive index of the sample (between 1.3 – 1.7 for most polymers).

As follows, at low wavenumbers (700 – 2000 cm^{-1}) a strong penetration of the beam into the sample (between 1.2 and 3.2 μm for the ZnSe – PET couple) is expected, while at high wavenumbers the depth of penetration is between 0.6 – 0.9 μm.

About the PET substrate, we found two characteristic absorption bands, corresponding to CH_2 stretching (2970 cm^{-1} and 2900 cm^{-1}). After the deposition of ppAAc films on the PET substrate, typical IR signatures of the OH stretching are found at 3600 cm^{-1}, 3435 cm^{-1} and 3242 cm^{-1}. These vibrations are well emphasised after deconvolution of the absorption spectrum with Gauss type peaks. In case of ppNVF films a strong peak attributed to NH stretching vibrations is observed at 3280 cm^{-1}. The large widths of absorption bands suggest overlapping of specific vibrations, due to different chemical environments.

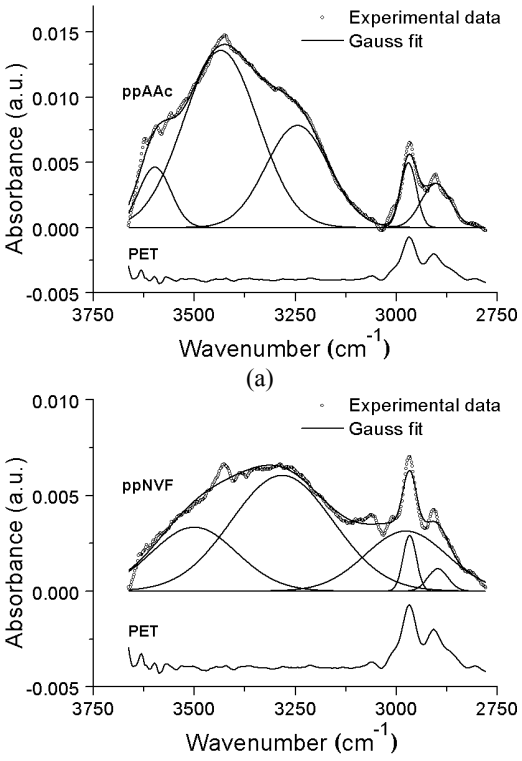

Fig. 7. Typical FTIR spectrum of the ppAAc (a) and ppNVF films (b)

In this step of our research, no information about the monomer structure during the plasma polymerization process are available. Due to the high energetic conditions induced by the DBD, a high fragmentation degree of the monomers and rearrangements of the fragments having functional groups incorporated are expected, leading to a 3D network of plasma polymer.

4. Conclusions

The experimental data proved that the dielectric barrier discharge is a simple and efficient technique in obtaining polymerized films onto the dielectric substrates. The spatial distribution of the total light emission intensity of the discharge showed that the highest energetic conditions are located near the dielectric substrate, favouring the monomer fragmentation and deposition onto the substrate. The plasma polymerized films comprise a good wettability due to the OH or NH radicals incorporated into the polymer matrix. These films are good candidates as substrates for immobilization of biological active agents, such as L-Asparaginase and other drugs.

References

[1] C. Monfardini, F. M. Veronese, Bioconjugate Chem **9**, 418 (1998).
[2] I. Vina, A. Karsakevich, M. Bekers, J. Mol. Catalysis B **11**, 551, (2001).
[3] S. D. Johnson, J.M. Anderson, R.E. Marchant , J. Biomed. Mater. Res. **26**, 915 (2004).
[4] P. K. Chu, J. Y. Chen, L. P. Wang, N. Huang N – Mater. Sci. Eng. R **36,** 143 (2002).
[5] L. Detomaso, R. Gristina, G. S. Senesi, R. d'Agostino P. Favia, Biomaterials **26**, 3831 (2005).
[6] C. Oehr, M. Müller, B. Elkin, D. Hegemann, U. Vohrer – Surf. Coat. Technol. **116**, 25 (1999).
[7] W. S. Rasband, "ImageJ", U.S. National Institutes of Health, 1997-2007, http://rsb.info.nih.gov/ij/.
[8] S. Liu, M. Neiger – J.Phys.D: Appl.Phys, **36**, 1565 (2003).
[9] A. S. Chiper, V. Anita, C. Agheorghiesei, V. Pohoata, M. Anita, G. Popa – Plasma Proc. Polym. **1**, 57 (2004).
[10] N. K. Bibinov, A.A. Fateev, K. Wiesemann – Plasma Sources Sci. Technol. **10**, 579 (2001).
[11] V. Poenariu, M.R. Wertheimer, R. Bartnikas – Plasma Proc. Polym. **3**, 17 (2006).
[12] J. L. Koenig (Ed.), Spectroscopy of polymers, Elsevier, (1999).

*Corresponding author: itopala@plasma.uaic.ro